

# Intermodal soliton interaction in nearly degenerate modes of a multimode fiber

SHAIVAL BUCH\* AND GOVIND P. AGRAWAL

The Institute of Optics, University of Rochester, Rochester, New York 14627, USA

\*Corresponding author: shaival.buch@rochester.edu

Received 14 July 2016; revised 13 September 2016; accepted 13 September 2016; posted 14 September 2016 (Doc. ID 270482); published 5 October 2016

We numerically investigate the interaction of two temporal solitons propagating in the two degenerate or nearly degenerate modes of a multimode fiber. Similar to the case of single-mode fibers, the solitons are found to attract or repel each other depending on their relative phase, even though they belong to two different modes of the fiber. However, unlike the single-mode case, each soliton transfers some of its power to the other mode through intermodal four-wave mixing. Our results show that, in spite of this intermodal power transfer, each soliton keeps propagating as a bimodal soliton and interacts with the other bimodal soliton as if they were propagating inside a single-mode fiber. Indeed, the total power in the two modes evolves similar to the case of a single-mode fiber. We study the impact of varying input parameters such as the relative phase, amplitude, and spacing of the two input pulses used to excite the fundamental solitons and point out differences introduced by the intermodal nature of the nonlinear effects. © 2016 Optical Society of America

**OCIS codes:** (190.4370) Nonlinear optics, fibers; (190.5530) Pulse propagation and temporal solitons.

<http://dx.doi.org/10.1364/JOSAB.33.002217>

## 1. INTRODUCTION

The study of nonlinear effects in multimode fibers (MMFs) is attracting considerable attention recently [1–18]. The renewed interest in MMFs is related to their potential applications in optical communications [19–23], image formation [24–26], and construction of high-power fiber lasers [8,9,27]. One of the important properties of nonlinear media is their ability to support solitary waves, or temporal solitons that are formed when the nonlinear effects exactly compensate for dispersion in the media. Propagation and interaction of temporal solitons inside a single-mode fiber (SMF) is well understood and is used for a variety of applications including supercontinuum generation [28].

The formation and evolution of solitons in MMFs is still not completely understood because of the complexity introduced by the simultaneous presence of multiple modes. Mathematically, a coupled set of nonlinear Schrödinger equations must be solved [1]. The complexity arises from the intermodal nonlinear coupling, which can lead to new and interesting nonlinear effects. Multimode solitons, in which energy of a single pulse is spread over several low-order modes, have been observed experimentally and studied theoretically [7,8]. Since such pulses are confined in both space and time, they are sometimes referred to as spatio-temporal solitons. In an earlier study, we studied the case in which fundamental solitons are launched simultaneously in several modes of a few-mode fiber and looked for conditions where

multiple solitons can propagate over long distances in a stable fashion [15]. Our study included differential group delay (DGD) and found that, under some conditions, solitons can trap each other and propagate with the same speed. Nonlinear coupling is generally stronger for modes that are degenerate or nearly degenerate. Indeed, soliton trapping ceased to occur for a large DGD.

In our previous study, two solitons launched simultaneously in two nearly degenerate modes overlapped temporally. In this paper, we consider the case when solitons are launched in such a way that they are separated initially with some overlap in the tail region, which still allows weak nonlinear coupling. The situation is similar to the study of soliton interaction in SMFs [29–39] with one main difference. In the case of SMFs, the two solitons overlap completely spatially as they share the same mode. In contrast, the two solitons propagate in different modes of a MMF and overlap only partially. Mathematically, we solve a set of coupled nonlinear equations numerically to simulate pulse evolution in MMFs. Our results show that, similar to the SMFs, soliton interaction in MMFs also depends on the relative phase of the two solitons. However, the multimode nature of the fiber also leads to several significant differences.

The paper is organized as follows. In Section 2 we present the numerical model and discuss the parameters used in numerical simulations. In Section 3 we focus on the case of two degenerate modes and study the effect of changing input parameters such as initial temporal separation of two solitons

and their relative amplitudes and phases. In Section 4 we study the more realistic case in which the two modes in which solitons are propagating have slightly different propagation constants and also exhibit some differential group delay. The main results are summarized in Section 5.

## 2. NUMERICAL MODEL

We consider an ideal MMF and assume that its modal spatial distributions  $F_m(x, y)$  and propagation constants  $\beta_m$  are known for all  $M$  modes ( $m = 1, 2, \dots, M$ ). In this study we ignore linear coupling among modes that often occurs in practice due to random perturbations in the refractive index [3–5]. We also assume that optical pulses can be selectively launched into any spatial mode of the MMF through a suitable mode-multiplexing device. In the frequency domain, the total electric field at any point  $z$  inside the fiber can be written as

$$\mathbf{E}(x, y, z, \omega) = \sum_{m=1}^M [\hat{x}\tilde{A}_{mx}(z, \omega) + \hat{y}\tilde{A}_{my}(z, \omega)]F_m(x, y)e^{i\beta_p(\omega)z}, \quad (1)$$

where  $\tilde{A}_{mx}(z, \omega)$  and  $\tilde{A}_{my}(z, \omega)$  are the spectral amplitudes of the  $x$ - and  $y$ -polarized components of  $m$ th mode, respectively. Maxwell's equations can be used to find an equation that describes evolution of these components inside a MMF [1–3,5]. We simplify this equation by not including the higher-order nonlinear (Raman and shock) terms as well as dispersion terms of order three and higher. We also convert it to the time domain and normalize it using the so-called soliton units. The resulting equation for the  $p$ th mode can be written as [15]

$$\begin{aligned} \frac{\partial \mathbf{u}_p}{\partial \xi} + d_{1p} \frac{\partial \mathbf{u}_p}{\partial \tau} + i \frac{d_{2p}}{2} \frac{\partial^2 \mathbf{u}_p}{\partial \tau^2} = iN_r^2 \\ \times \sum_l \sum_m \sum_n f_{lmnp} \left[ \frac{2}{3} (\mathbf{u}_l^H \mathbf{u}_m) \mathbf{u}_n + \frac{1}{3} (\mathbf{u}_n^T \mathbf{u}_m) \mathbf{u}_l^* \right] e^{i(\Delta\phi_{lmnp}\xi)}, \end{aligned} \quad (2)$$

where  $\mathbf{u}_p = \mathbf{A}_p / \sqrt{P_r}$ ,  $\mathbf{A}_p = [A_{px}, A_{py}]^T$  is a Jones vector, and  $A_{px}$  is the slowly varying envelope of the  $x$ -polarized pulse propagating in  $p$ th spatial mode of the fiber. The superscripts  $T$  and  $H$  stand for the transpose and Hermitian conjugate of a matrix. The power  $P_r$  used to normalize the amplitude is the peak power needed to form a fundamental soliton in a specific (reference) mode of the fiber.

In deriving Eq. (2), the propagation constant  $\beta_p$  of each mode was expanded in a Taylor series as

$$\beta_p(\omega) = \beta_{0p} + \beta_{1p}(\omega - \omega_0) + \beta_{2p}(\omega - \omega_0)^2/2 + \dots, \quad (3)$$

where  $\beta_{kp} = (d^k \beta_p / d\omega^k)|_{\omega=\omega_0}$ . The parameters  $d_{1p}$  and  $d_{2p}$  are defined as

$$d_{1p} = (\beta_{1p} - \beta_{1r})L_{dr}/T_0, \quad d_{2p} = \beta_{2p}/|\beta_{2r}|. \quad (4)$$

In soliton units  $\xi = z/L_{dr}$  is the distance normalized using the dispersion length defined as  $L_{dr} = T_0^2/|\beta_{2r}|$  and  $\tau = (t - \beta_{1r}z)/T_0$  is the reduced time, where  $T_0$  is related to the width of input pulses. The phase mismatch on the right side of Eq. (2) is given by  $\Delta\phi_{lmnp} = (\beta_{0m} + \beta_{0n} - \beta_{0l} - \beta_{0p})L_{dr}$ .

The nonlinear effects in Eq. (2) are included through the soliton order  $N_r$  defined as  $N_r^2 = \gamma P_r T_0^2 / |\beta_{2r}|$ , where  $\gamma =$

$n_2\omega_0/(cA_1^{\text{eff}})$  is the nonlinear parameter of the fiber with the effective area  $A_1^{\text{eff}}$  of the fundamental mode and  $n_2$  is the Kerr parameter. The strength of intermodal nonlinear coupling is governed by the dimensionless quantity  $f_{lmnp}$  given by

$$f_{lmnp} = A_1^{\text{eff}} \iint F_l^* F_m F_n F_p^* dx dy, \quad (5)$$

where  $F_m(x, y)$  is the spatial distribution of the  $m$ th mode, assumed to be normalized such that  $\iint |F_m|^2(x, y) dx dy = 1$ .

We apply Eq. (2) to a graded-index fiber supporting three spatial modes, referred to as LP<sub>01</sub>, LP<sub>11a</sub> and LP<sub>11b</sub>, and label them with  $m = 1, 2, 3$ , respectively. It is well known that the LP<sub>11a</sub> and LP<sub>11b</sub> modes are almost degenerate in an optical fiber and become degenerate in the weakly guiding approximation. We first assume that this approximation holds and use  $\beta_2 = \beta_3$ . In this paper we study the case when input pulses are launched in these two modes with enough peak powers to form a fundamental soliton at wavelength  $\lambda_0$ . Using mode 2 as the reference mode and assuming no power in the mode 1, Eq. (2) leads to the following set of coupled equations:

$$\begin{aligned} \frac{\partial \mathbf{u}_2}{\partial \xi} + i \frac{d_{22}}{2} \frac{\partial^2 \mathbf{u}_2}{\partial \tau^2} = iN_2^2 \\ \times [f_{2222} |\mathbf{u}_2|^2 \mathbf{u}_2 + (f_{3322} + f_{3232}) |\mathbf{u}_3|^2 \mathbf{u}_2 + f_{2332} \mathbf{u}_3^* \mathbf{u}_2^*], \end{aligned} \quad (6a)$$

$$\begin{aligned} \frac{\partial \mathbf{u}_3}{\partial \xi} + i \frac{d_{23}}{2} \frac{\partial^2 \mathbf{u}_3}{\partial \tau^2} = iN_3^2 \\ \times [f_{3333} |\mathbf{u}_3|^2 \mathbf{u}_3 + (f_{2233} + f_{2323}) |\mathbf{u}_2|^2 \mathbf{u}_3 + f_{3223} \mathbf{u}_2^* \mathbf{u}_3^*]. \end{aligned} \quad (6b)$$

These equations still include both polarizations for each mode. The first-order time derivatives do not appear in them because the group velocity is the same for all four modes ( $d_{12} = d_{13} = 0$ ). We solve them numerically with the well-known split-step Fourier method [28] using the parameters given in Table 1. We even include mode 1 in our simulations to capture any potential transfer of energy to this initially unexcited mode through nonlinear mechanisms, such as intermodal four-wave mixing (FWM) and modulation instability induced by cross-phase modulation [28]. It is important to stress that the numerical model is valid for any MMF, including a highly multimodal graded-index fiber. Hence, our results and conclusions should apply qualitatively even for such fibers as long as only two nearly degenerate modes of the fiber are being initially excited.

**Table 1. Parameters Used for Numerical Modeling**

Parameter Group	Values
Nonlinearity	$\gamma = 1.77 \text{ W}^{-1}/\text{km}$ $f_{1111} = 1, f_{2222} = f_{3333} = 1/2$ $f_{2233} = f_{3322} = f_{2323} = 1/4$ $f_{2332} = f_{3232} = f_{3223} = 1/4$
Dispersion	$\beta_{22} = \beta_{23} = 24.3 \text{ ps}^2/\text{km}$
Pulse	$T_0 = 1 \text{ ps}, P_r = 18.38 \text{ W}, \lambda_0 = 1540 \text{ nm}$

Before considering the MMF case we briefly review the expected behavior when two temporally separated solitons interact nonlinearly inside a SMF. If the initial separation is not too large, the tails of the two solitons overlap partially and they either attract or repel each other depending on their relative phase. In particular, two in-phase identical solitons attract each other until they collide at a distance known as the collision distance. After that, they cross over and recover their initial separation, and the whole procedure repeats in a periodic fashion. Even small changes in the solitons' relative amplitudes or phases affect this scenario drastically, and the solitons may repel each other if such changes are large enough.

### 3. SOLITON INTERACTION IN TWO FIRST-ORDER DEGENERATE MODES

In this section we focus on the  $LP_{11a}$  and  $LP_{11b}$  modes of a MMF and assume that they are fully degenerate ( $\beta_2 = \beta_3$ ). We also assume that both solitons remain linearly polarized along the  $x$  direction as they propagate inside a MMF and set  $u_{2y} = u_{3y} = 0$ . We further assume that input pulses have the same widths and peak powers and choose  $N_2 = N_3 = 1$  with

$$u_{2x}(0, \tau) = \text{sech}(\tau - q_0), \quad u_{3x}(0, \tau) = \text{sech}(\tau + q_0)e^{i\theta}, \quad (7)$$

where  $\theta$  is relative phase shift. If  $T_s$  is initial temporal separation of the two pulses launched to excite the two solitons,  $2q_0 = T_s/T_0$ . If  $q_0$  is not too large, the tails of the two solitons will partially overlap, and the two solitons will interact nonlinearly, even though they belong to different fiber modes, because their spatial modes also partially overlap.

#### A. Interaction of Two In-Phase Solitons

We choose  $T_0 = 1$  ps,  $q_0 = 4$ , and  $\theta = 0$ , representing two in-phase fundamental solitons separated by 8 ps initially. The dispersion length ( $L_d$ ) is about 40 m in this case. The first two panels of Fig. 1 show the evolution of mode powers over  $100L_d$ , while the third panel shows the total power in the two modes. Similar to the case of SMFs, two solitons attract each other (through intermodal nonlinear coupling) and move toward each other, even though they belong to two different modes of the fiber. However, unlike the single-mode case, we find that each soliton transfers some of its power to the other mode as the two solitons approach each other. Eventually the two solitons overlap completely, forming an intense bimodal pulse at a distance of about  $75L_d$ . At this point, each pulse is considerably narrower than the input pulse and its spectrum is also wider. With further propagation, both pulses cross over and separate from each other, almost returning to their original separation after  $150L_d$ . However, we stress that the input conditions are never recovered fully because some energy remains in the original time slot.

Intermodal soliton interaction in Fig. 1 is similar to that occurring in SMFs with some obvious differences. The major difference is that there is an intermodal exchange of power during the initial attraction phase. The underlying physical mechanism behind power transfer is the intermodal FWM, governed by the last term in Eqs. (6a) and (6b), which causes a part of the energy from one mode to be transferred to the other mode. If

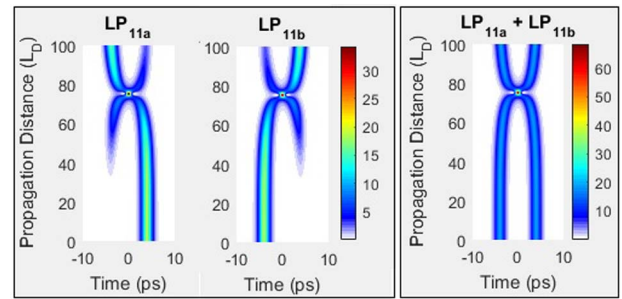


**Fig. 1.** Interaction of two temporally separated solitons launched in degenerate modes. (Left) Evolution of power in individual modes. (Right) Sum of powers in both modes. The color bar shows optical power on a linear scale.

we plot the powers in Fig. 1 on a logarithmic scale, we note that power transfer begins right after pulses are launched but it becomes a noticeable fraction of the peak power in Fig. 1 only after  $30L_d$  or so.

Figure 2 shows the evolution of the power in mode 2 in the range  $60\text{--}85L_d$  that includes the point at which two solitons “collide” and overlap temporally; power variations in mode 3 are just a mirror image of Fig. 2 around  $\tau = 0$ . The smaller peak on the left is due to the intermodal power transfer. One can see that it grows in amplitude, while the other on the right weakens, because of a continuous transfer of power to the other mode. The reason why this peak also moves toward the center is that it is trapped by the soliton in mode 3 through intermodal cross-phase modulation. Even after the point of collision, once the pulses cross over and start to separate temporally, a small portion of the energy in mode 2 stays trapped with the pulse propagating in mode 3 (and vice versa). However, if we add the powers in the two modes, the interaction appears to be virtually indistinguishable from the case of SMFs (last panel in Fig. 1). This is surprising but also reassuring since total energy of the two solitons must be conserved in the absence of losses. It is not obvious why the two-mode interaction should mimic the single-mode case when intensities (rather than

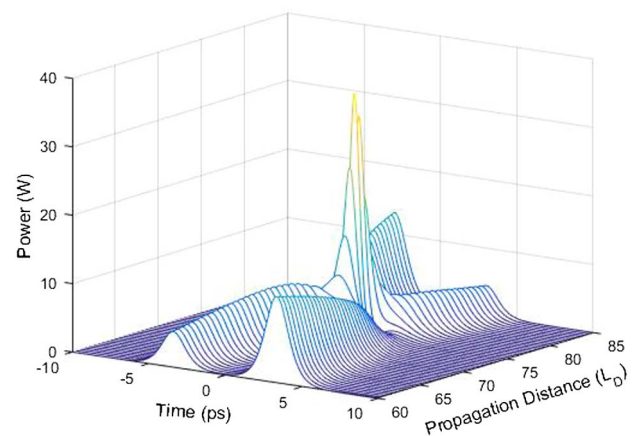


**Fig. 2.** Magnified view of the  $LP_{11a}$  mode power in a range that includes the point of collision. The peak initially on the left is due to intermodal power transfer from the  $LP_{11b}$  mode.

amplitudes) are added together. The similarity between the SMF case and the degenerate modes of a MMF has also been noted in the strong mode-coupling regime [3].

One way to understand the features seen in Figs. 1 and 2 is in terms of the concept of a multimode soliton [7,8] whose energy is distributed over several modes that are locked with each other and propagate as one unit as a “spatiotemporal” soliton. In this picture, even though a part of each soliton’s energy is transferred to the other degenerate mode, both parts remain part of the same “bimodal” soliton. Since the modes are assumed to be perfectly degenerate, the exchange of power due to intermodal FWM is equal in both directions and hence the total energy in each mode is conserved. Intermodal FWM appears to be distinct from intra-channel FWM studied in the context of telecommunication systems [40,41] because of the absence of ghost pulses.

### B. Impact of Relative Phases and Amplitudes of Solitons

First, we study how the intermodal soliton interaction depends on the relative phase shift  $\theta$ . As mentioned earlier, soliton interaction is quite sensitive to  $\theta$  in the case of SMFs. For this reason, we expect qualitative changes to occur with changes in  $\theta$  even in MMFs. Figure 3 shows the effect of changing  $\theta$  while keeping the same value  $q_0 = 4$  for the initial temporal separation. For  $\theta = \pi/8$  (top row) and  $\pi/4$  (middle row), the solitons still experience intermodal attraction initially, but they separate from

each other and never appear to collide. Indeed, the last panels where total power in the two modes is plotted exhibit features that are almost identical to the single-mode case.

However, when we look at the mode powers in each mode individually, we find new remarkable features. Intermodal power transfer similar to that seen in Fig. 1 still occurs and it does depend to some extent on the exact value of  $\theta$ . Around  $75L_D$ , the distance where solitons crossed over in the in-phase case, we observe that, despite the absence of complete temporal overlap of the two solitons, the entire mode power has shifted temporally to the other side. This feature is hard to understand. One possibility is that intermodal FWM becomes so strong that it transfers the entire power in mode 2 to mode 3 (and vice versa). A second possibility is to invoke the formation of multimode solitons and only consider the sum of powers in the two modes as a relevant quantity.

Another remarkable feature in Fig. 3 is the temporal asymmetry seen clearly in the last panel of the top row. Notice how the trace on the left is more intense than on the right after the two pulses separate from each other. Thus, even if we interpret the soliton interaction in terms of multimode solitons, intermodal FWM is not symmetric when  $\theta \neq 0$ . More power is transferred to the soliton on the left, making it more intense. This asymmetry is also present in individual mode powers. If we look carefully, the direction of power transfer is not uniform, which leads to one mode having more energy compared to the other mode. In other words, the energy in each mode is no longer conserved, although the total energy remains conserved.

We have verified that this asymmetry occurs even in the case of single-mode fibers and is related to the sign of the phase difference  $\theta$ . Indeed, when we change the sign such that  $\theta = -\pi/8$ , we find that the direction of power transfer is reversed such that the soliton on the right is more intense than on the left, in contrast to what is seen in the top panel of Fig. 3. This means that not only the magnitude of the relative phase but also its sign plays a role in deciding which mode is preferred by intermodal FWM.

The bottom row in Fig. 3 shows the case of  $\theta = \pi/2$ . For this specific value of  $\theta$  both solitons appear to propagate, without any interaction or intermodal FWM, as if the other soliton did not even exist. This behavior is quite different than what is observed in SMFs. In that case, solitons experience repulsion and move away from each other when  $\theta = \pi/2$ . The physical reason why the multimode case is so different for this specific value of  $\theta$  is not understood at this time. One factor that may contribute to this difference is the partial spatial overlap between the two modes compared to the SMF case where the overlap is 100%.

We also change  $q_0$  by varying the initial temporal separation between the pulses. The first plot in Fig. 4 shows how the spacing between the two solitons changes as they propagate down the fiber for three values of  $\theta$  while choosing  $q_0 = 4$ . The spacing goes to zero only for  $\theta = 0$  at a certain distance where the two solitons overlap fully (or collide). In the case of  $\theta = 0$  the qualitative behavior remains identical to that seen in Fig. 1 for other values of  $q_0$  except that the two solitons collide after a shorter distance for smaller values of  $q_0$ . This dependence on  $q_0$  is shown in the second plot in Fig. 4. Similar to the single-mode case, the collision distance depends exponentially on  $q_0$ , as verified by an exponential fit to the numerical data (dashed line).

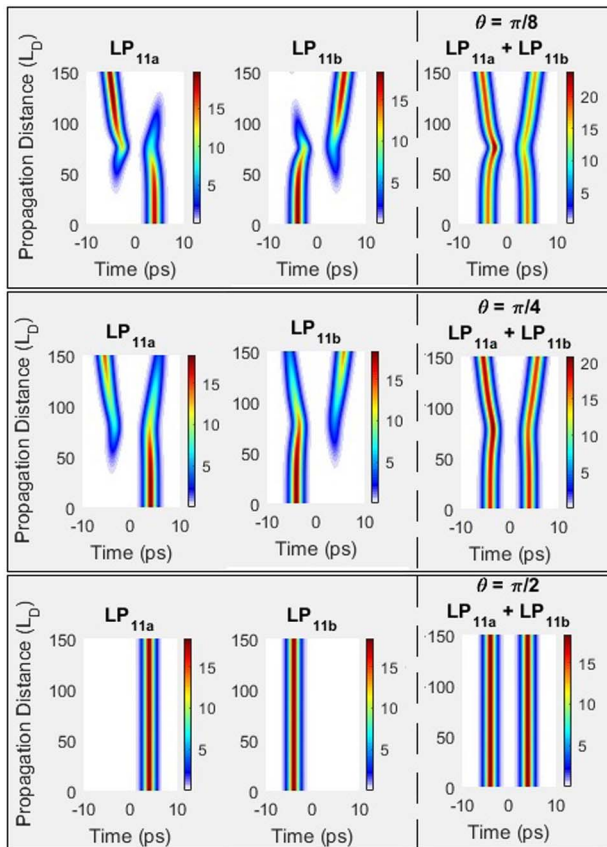


**Fig. 3.** Effects of initial phase difference on intermodal soliton interaction: (top row)  $\theta = \pi/8$ , (middle row)  $\theta = \pi/4$ , (bottom row)  $\theta = \pi/2$ . Power is color-coded on a linear scale.

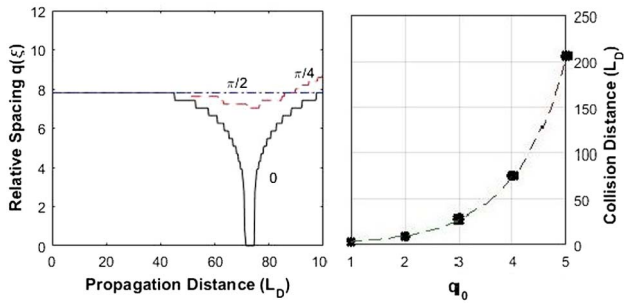


**Fig. 4.** (left) Spacing between the two solitons as a function of propagation distance for three values of  $\theta$ . (right) Dependence of collision distance on the initial pulse separation for two in-phase solitons. The dashed line shows an exponential fit to the numerical data.

In the single-mode case, nonlinear interaction also depends on the relative amplitudes of two solitons [28]. We studied the amplitude dependence in the two-mode case by changing the peak powers that affect the soliton orders  $N_2$  and  $N_3$  associated with the two pulses. To emphasize the bimodal nature of the solitons, Fig. 5 shows how the total power in the two modes varies over  $100L_d$  for the case of  $N_2 = 1$  and  $N_3 = 1.1$  after choosing  $q_0 = 4$  and  $\theta = 0$ . In contrast to the equal-amplitude case shown in Fig. 1, the two bimodal solitons never collide and exhibit an oscillatory behavior with the distance. These results indicate that the amplitudes and phase of the two input pulses can thus be used to control the interaction process in MMFs.

One may ask whether the periodic evolution of two in-phase solitons over long distances predicted in the case of SMFs holds in the case of MMFs. To answer this question, we reduce the initial separation  $2q_0$  between the two solitons so that they collide at a much shorter distance and propagate them long enough to record several collisions. Figure 6 shows the results by plotting the evolution of bimodal solitons for  $q_0 = 2$  and 3. Clearly, intermodal interaction of two in-phase solitons inside a MMF is far from being periodic. As seen in Fig. 6, successive collisions occur after increasingly shorter distances. This breakdown in periodicity is certainly a consequence of the

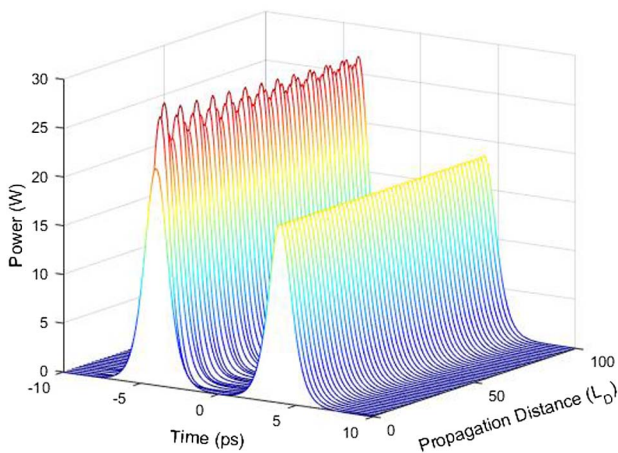


**Fig. 5.** Intermodal interaction of two in-phase solitons of the same width with different amplitudes ( $N_2 = 1, N_3 = 1.1$ ). Total power in both modes is plotted as a function of distance.

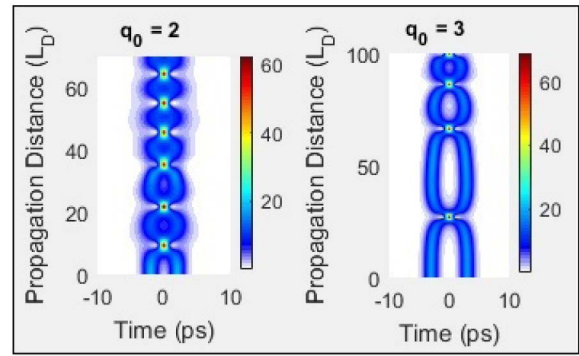


**Fig. 6.** Breakdown of periodicity in MMFs in collisions of two in-phase solitons. Total power in the two degenerate modes is plotted as a function of distance for  $q_0 = 2$  and 3 with color-coding on a linear scale.

intermodal FWM among the modes. Because of this phenomenon, after the first collision, each mode has two pulses propagating through it, one of which is the original soliton launched into that mode and the other forms due to energy transfer from the other mode. As a result, each pulse experiences not only intermodal nonlinear coupling, but also intramodal nonlinear coupling, and the initial launch conditions are not reproduced after the first collision. It is thus not surprising that the distances at which the second and later collisions occur are different than that of the first collision.

#### 4. CASE OF TWO NEARLY DEGENERATE MODES

In this section we investigate how the intermodal interaction changes when the two modes are not exactly degenerate ( $\beta_2 \neq \beta_3$ ). One expects the results of Section 3 to hold qualitatively for relatively small deviations, and the question is how much deviations are tolerable. Since  $\beta_2$  is not expected to change much for small deviations, we answer this question numerically by introducing two parameters defined as  $\Delta\beta_0 = \beta_{02} - \beta_{03}$  and  $\Delta\beta_1 = \beta_{12} - \beta_{13}$ , the latter representing the DGD between the two nearly degenerate modes.

Figure 7(a) shows the evolution of individual mode powers and total bimodal power over  $300L_d$  under conditions identical to those in Fig. 1, except that  $\Delta\beta_0$  now has a finite value of  $0.1 \text{ m}^{-1}$ . The bimodal picture shows an initial attraction phase leading to a near collision of the two bimodal solitons around  $75L_d$  after which they separate from each other. The individual mode powers, however, show even more drastic changes caused by slightly different propagation constants. After the first collision, each mode repetitively transfers power to the other mode forth and back, but the two modes do not behave in a symmetric fashion. Indeed, as seen in Fig. 7(a) the  $LP_{11a}$  mode becomes more intense compared to the other mode after the attraction phase. Similar to the case of initial phase difference  $\theta$  studied in Section 3, the sign of  $\Delta\beta_0$  determines which mode is preferred. When we reverse the sign and make  $\Delta\beta_0$  negative, it is the  $LP_{11b}$  mode that becomes more intense, and the total bimodal power exhibits a pattern that is the mirror image of the one seen in Fig. 7(a).

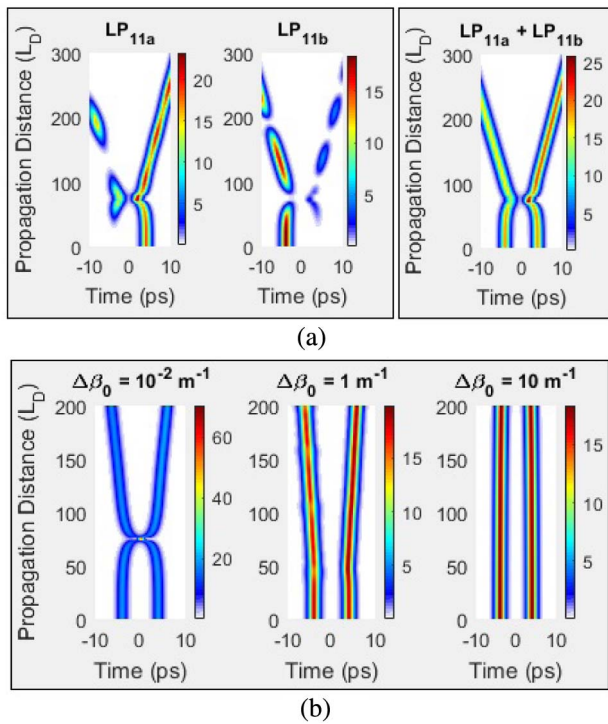


**Fig. 7.** Interaction of two in-phase solitons propagating in nearly degenerate modes with parameters identical to those used in Fig. 1. (a) Evolution of individual mode powers and total bimodal power over  $300L_d$  for  $\Delta\beta_0 = 0.1 \text{ m}^{-1}$ . (b) Total power in both modes for three values of  $\Delta\beta_0$ .

To quantify the tolerable values of  $\Delta\beta_0$ , Fig. 7(b) shows the evolution of total bimodal power over  $200L_d$  for three values of  $\Delta\beta_0$  ranging from  $0.01$  to  $10 \text{ m}^{-1}$  using the same parameters used in Fig. 7(a). For the smallest value of  $\Delta\beta_0$ , the initial behavior is similar to the case of degenerate modes shown in Fig. 1. The two solitons attract each other and collide after almost the same distance as in Fig. 1. But even for this small value of  $\Delta\beta_0$ , the behavior after the first collision is different since the two bimodal solitons repel each other and do not collide again. Further increasing  $\Delta\beta_0$  leads to weaker nonlinear coupling between the modes, and even the initial collision ceases to occur. After  $\Delta\beta_0$  exceeds  $5 \text{ m}^{-1}$ , the two bimodal solitons propagate independently as if they were isolated from each other. We thus conclude that the intermodal collision of two in-phase solitons requires the ratio  $|\Delta\beta_0|/\beta_{02}$  to be below  $10^{-7}$ , making it unlikely that it can be observed in practical fibers.

Finally, we study the impact of modal DGD on soliton interaction. Figure 8 shows soliton interaction for different values of  $\Delta\beta_1$ . The modes are assumed to have the same propagation constant. Although this situation is not realized in practice, it is simulated to isolate the effects of DGD on intermodal interaction of solitons. In Fig. 8(a), we show the behavior of solitons in individual modes as well as that of two bimodal solitons for  $\Delta\beta_1 = 3 \text{ ps/km}$ . As seen there, the individual solitons change their group velocity, one of them speeding up while the other slows down, under the influence of nonlinear

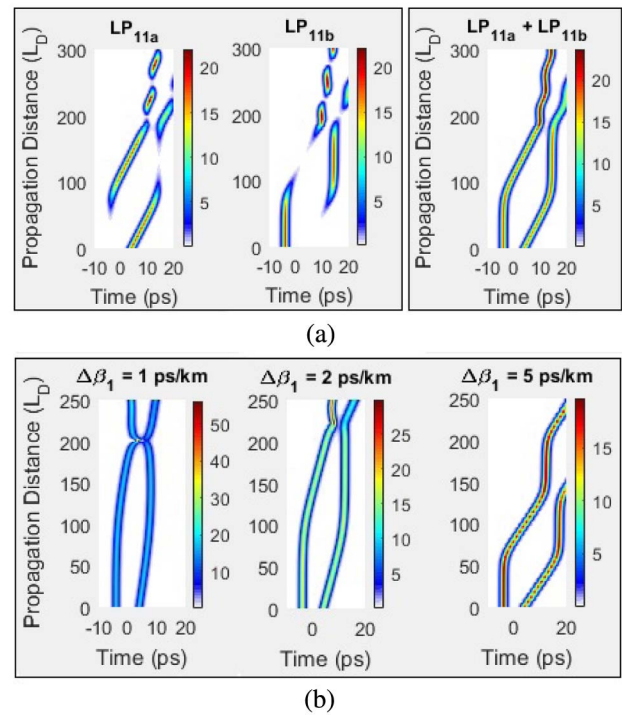


**Fig. 8.** Impact of DGD on the interaction of two in-phase solitons launched with  $q_0 = 4$ . (a) Evolution of individual mode powers and total bimodal power over  $300L_d$  for  $\Delta\beta_1 = 3 \text{ ps/km}$ . (b) Total power in both modes for three different values of DGD.

coupling. We also observe power being transferred repeatedly from one mode to the other. The last panel shows how the bimodal solitons attract each other after they have adjusted their speeds and nearly collide with each other. After the collision, one of the solitons becomes more intense. Again, the sign of  $\Delta\beta_1$  determines which mode is preferred.

Figure 8(b) shows the bimodal picture by summing the powers in the two modes for three values of  $\Delta\beta_1$  ranging from 1 to 5 ps/km. For a small value of DGD, the solitons exhibit a behavior quite similar to that seen in Fig. 1 (no DGD). More specifically, they adjust their speeds quickly to travel at the same speed and collide after some distance because of an attraction between two bimodal in-phase solitons. In this scenario, the two solitons qualitatively exhibit interaction behavior similar to the no-DGD case, except that the distance at which they collide is longer than that in Fig. 1. As the magnitude of  $\Delta\beta_1$  increases, the nonlinear coupling keeps getting weaker, and the collision distance keeps increasing. After a certain value, the nonlinear coupling weakens enough that the solitons no longer undergo collision. For DGD values beyond 10 ps/km, the two solitons do not interact with each other as the pulses cease to have any temporal overlap soon after they are launched.

## 5. CONCLUSIONS

We studied numerically the interaction of two temporal solitons propagating in the two degenerate or nearly degenerate modes of a MMF. Similar to the case of a SMF, the solitons are found to attract or repel each other depending on their

relative phase, even though they belong to two different modes of the fiber. However, unlike the single-mode case, each soliton transfers some of its power to the other mode through intermodal FWM. Our results show that, in spite of this intermodal power transfer, each soliton keeps propagating as a bimodal soliton and interacts with the other bimodal soliton as if they were propagating inside a SMF. Indeed, when the modes are fully degenerate, the total power in the two modes evolves in a fashion identical to the case of a SMF.

In the degenerate case, we studied in detail the impact of varying input parameters, such as the relative phase, amplitude, and spacing of the two input pulses used to excite the fundamental solitons. In all cases, bimodal solitons form because of intermodal power transfer through FWM that interact with each other and exhibit features similar to those occurring in a SMF with one important difference. In the multimode case, the evolution of bimodal solitons does not coincide with the single-mode case over long distances. Even two identical in-phase solitons do not exhibit a periodic behavior such that they collide again and again after the same distance. Rather, we found that the successive collisions occur after shorter and shorter distances.

In the nearly degenerate case, we studied how small changes in the modal propagation constants, or group velocities, affected the intermodal interaction between two solitons. We found that the difference  $\Delta\beta_0$  between the modal propagation constants should be a small fraction of the average value ( $<10^{-7}$  for the qualitative behavior to remain identical to the degenerate case). In the case of DGD,  $\Delta\beta_1$  values of  $<1$  ps/km do not affect the intermodal interaction qualitatively but the two solitons cease to interact when  $\Delta\beta_1$  exceeds 10 ps/km.

One may ask whether the intermodal interaction of optical pulses studied in this paper can be observed using realistic fibers. Simple calculations show that the value of  $\Delta\beta_0$  between any two adjacent modes of a commercially available graded-index MMF (core diameter  $>50$   $\mu\text{m}$ ) is at least 2 orders of magnitude larger than the tolerable value of  $\Delta\beta_0$  found here. However, three-mode fibers designed with a core diameter just large enough that the two nearly degenerate first-order modes exist, in addition to the fundamental mode, are a potential candidate, provided their core-cladding index difference is small enough that the weakly guiding approximation holds. Both  $\Delta\beta_0$  and  $\Delta\beta_1$  for such fibers are expected to be small enough that the theoretical predictions of this paper should be verifiable. Another possibility is to employ two orthogonally polarized modes belonging to the same spatial mode of a fiber designed with low birefringence. We have verified that all features of the intermodal interaction of optical pulses studied in this paper occur even in this situation.

It is important to stress that the effects described here are solely dependent on the nonlinear coupling among modes of an ideal fiber since we have ignored all sources of linear coupling between the mode pairs. In practice, linear coupling among fiber modes owing to random refractive-index perturbations is hard to avoid [3–5]. Since degenerate modes are likely to have a much shorter coupling length compared to the dispersion and nonlinear length scales (strong coupling regime), some of the effects described here may be hard to

observe. As the dispersion and nonlinear lengths can be reduced considerably by using ultrashort pulses with high peak powers, their use together with MMFs exhibiting weak linear coupling is recommended for experimental verification. Our study is useful for a fundamental understanding of the formation, evolution, and interaction of optical solitons in few-mode fibers.

**Funding.** National Science Foundation (NSF) (ECCS-1505636).

**Acknowledgment.** The authors would like to thank Dr. René-Jean Essiambre for important discussions and insights.

## REFERENCES

1. F. Poletti and P. Horak, "Description of ultrashort pulse propagation in multimode optical fibers," *J. Opt. Soc. Am. B* **25**, 1645–1654 (2008).
2. A. Mafi, "Pulse propagation in a short nonlinear graded-index multimode optical fiber," *J. Lightwave Technol.* **30**, 2803–2811 (2012).
3. A. Mecozzi, C. Antonelli, and M. Shtaif, "Nonlinear propagation in multi-mode fibers in the strong coupling regime," *Opt. Express* **20**, 11673–11678 (2012).
4. A. Mecozzi, C. Antonelli, and M. Shtaif, "Coupled Manakov equations in multimode fibers with strongly coupled groups of modes," *Opt. Express* **20**, 23436–23441 (2012).
5. S. Mumtaz, R.-J. Essiambre, and G. P. Agrawal, "Nonlinear propagation in multimode and multicore fibers: generalization of the Manakov equations," *J. Lightwave Technol.* **31**, 398–406 (2013).
6. R.-J. Essiambre, M. A. Mestre, R. Ryf, A. H. Gnauck, R. W. Tkach, A. R. Charplyvy, Y. Sun, X. Jiang, and R. Lingle, "Experimental investigation of inter-modal four-wave mixing in few-mode fibers," *IEEE Photon. Technol. Lett.* **25**, 539–542 (2013).
7. W. H. Renninger and F. W. Wise, "Optical solitons in graded-index multimode fibers," *Nat. Commun.* **4**, 1719 (2013).
8. L. Wright, W. H. Renninger, D. N. Christodoulides, and F. W. Wise, "Spatiotemporal dynamics of multimode optical solitons," *Opt. Express* **23**, 3492–3506 (2015).
9. L. Wright, D. N. Christodoulides, and F. W. Wise, "Controllable spatiotemporal nonlinear effects in multimode fibres," *Nat. Photonics* **9**, 306–310 (2015).
10. L. Wright, S. Wabnitz, D. N. Christodoulides, and F. W. Wise, "Ultrabroadband dispersive radiation by spatiotemporal oscillation of multimode waves," *Phys. Rev. Lett.* **115**, 223902 (2015).
11. L. Wright, Z. Liu, D. A. Nolan, M.-J. Li, D. N. Christodoulides, and F. W. Wise, "Self-organized instability in graded-index multimode fibre," arXiv:1603.07414 (2016).
12. A. Picozzi, G. Millot, and S. Wabnitz, "Nonlinear optics: nonlinear virtues of multimode fibre," *Nat. Photonics* **9**, 289–291 (2015).
13. E. Nazemosadat, H. Pourbeyram, and A. Mafi, "Phase matching for spontaneous frequency conversion via four-wave mixing in graded-index multimode optical fibers," *J. Opt. Soc. Am. B* **33**, 144–150 (2016).
14. H. Pourbeyram, G. P. Agrawal, and A. Mafi, "Stimulated Raman scattering cascade spanning the wavelength range of 523 to 1750 nm using a graded-index multimode optical fiber," *Appl. Phys. Lett.* **102**, 201107 (2013).
15. S. Buch and G. P. Agrawal, "Soliton stability and trapping in multimode fibers," *Opt. Lett.* **40**, 225–228 (2015).
16. M. Guasoni, "Generalized modulational instability in multimode fibers: Wideband multimode parametric amplification," *Phys. Rev. A* **92**, 033849 (2015).
17. K. Krupa, A. Tonello, B. M. Shalaby, M. Fabert, A. Barthélémy, G. Millot, S. Wabnitz, and V. Couderc, "Spatial beam self-cleaning in multimode fiber," arXiv:1603.02972 (2016).
18. K. Krupa, A. Tonello, A. Barthélémy, V. Couderc, B. M. Shalaby, A. Bendahmane, G. Millot, and S. Wabnitz, "Observation of geometric parametric instability induced by the periodic spatial self-imaging of multimode waves," *Phys. Rev. Lett.* **116**, 183901 (2016).

19. D. J. Richardson, J. M. Fini, and L. E. Nelson, "Space-division multiplexing in optical fibers," *Nat. Photonics* **7**, 354–362 (2013).
20. G. Li, N. Bai, N. Zhao, and C. Xia, "Space-division multiplexing: the next frontier in optical communication," *Adv. Opt. Photon.* **6**, 413–487 (2014).
21. C. Antonelli, A. Mecozzi, M. Shtaif, and P. J. Winzer, "Stokes-space analysis of modal dispersion in fibers with multiple mode transmission," *Opt. Express* **20**, 11718–11733 (2012).
22. J. Carpenter, B. J. Eggleton, and J. Schröder, "Observation of Eisenbud-Wigner-Smith states as principal modes in multimode fibre," *Nat. Photonics* **9**, 751–757 (2015).
23. G. Milione, D. A. Nolan, and R. R. Alfano, "Determining principal modes in a multimode optical fiber using the mode dependent signal delay method," *J. Opt. Soc. Am. B* **32**, 143–149 (2015).
24. R. N. Mahalati, R. Y. Gu, and J. M. Kahn, "Resolution limits for imaging through multi-mode fiber," *Opt. Express* **21**, 1656–1668 (2013).
25. M. Plöschner, T. Tyc, and T. Čižmár, "Seeing through chaos in multimode fibres," *Nat. Photonics* **9**, 529–535 (2015).
26. E. E. Morales-Delgado, D. Psaltis, and C. Moser, "Two-photon imaging through a multimode fiber," *Opt. Express* **23**, 32158–32170 (2015).
27. E. Nazemosadat and A. Mafi, "Nonlinear switching in multicore versus multimode waveguide junctions for mode-locked laser applications," *Opt. Express* **21**, 30739–30745 (2013).
28. G. P. Agrawal, *Nonlinear Fiber Optics*, 5th ed. (Academic, 2013).
29. J. P. Gordon, "Interaction forces among solitons in optical fibers," *Opt. Lett.* **8**, 596–598 (1983).
30. B. Hermansson and D. Yevick, "Numerical investigation of soliton interaction," *Electron. Lett.* **19**, 570–571 (1983).
31. K. J. Blow and N. J. Doran, "Bandwidth limits of nonlinear (soliton) optical communication systems," *Electron. Lett.* **19**, 429–430 (1983).
32. D. Anderson and M. Lisak, "Bandwidth limits due to incoherent soliton interaction in optical-fiber communication systems," *Phys. Rev. A* **32**, 2270–2274 (1985).
33. D. Anderson and M. Lisak, "Bandwidth limits due to mutual pulse interaction in optical soliton communication systems," *Opt. Lett.* **11**, 174–176 (1986).
34. Y. Kodama and K. Nozaki, "Soliton interaction in optical fibers," *Opt. Lett.* **12**, 1038–1040 (1987).
35. C. Desem and P. L. Chu, "Soliton propagation in the presence of source chirping and mutual interaction in single-mode optical fibres," *Electron. Lett.* **23**, 260–262 (1987).
36. C. Desem and P. L. Chu, "Soliton interaction in the presence of loss and periodic amplification in optical fibers," *Opt. Lett.* **12**, 349–351 (1987).
37. C. Desem and P. L. Chu, "Reducing soliton interaction in single-mode optical fibres," *IEE Proc. Optoelectron.* **134**, 145–151 (1987).
38. F. M. Mitschke and L. F. Mollenauer, "Experimental observation of interaction forces between solitons in optical fibers," *Opt. Lett.* **12**, 355–357 (1987).
39. T. Georges and F. Favre, "Modulation, filtering, and initial phase control of interacting solitons," *J. Opt. Soc. Am. B* **10**, 1880–1889 (1993).
40. R.-J. Essiambre, B. Mikkelsen, and G. Raybon, "Intra-channel cross-phase modulation and four-wave mixing in high-speed TDM systems," *Electron. Lett.* **35**, 1576–1578 (1999).
41. P. V. Mamyshev and N. A. Mamysheva, "Pulse-overlapped dispersion-managed data transmission and intrachannel four-wave mixing," *Opt. Lett.* **24**, 1454–1456 (1999).